Transforming anion instability into stability: Contrasting photoionization of three protonation forms of the phosphate ion upon moving into water

Eva Pluhařová,[a,b] Milan Ončák,[b] Robert Seidel,[d,e] Christi Schroeder,[e] William Schroeder,[e] Bernd Winter,[d] Stephen E. Bradforth,[e] Pavel Jungwirth,[a] and Petr Slavíček[b,c,*]

[a]*Institute of Organic Chemistry and Biochemistry, Academy of Sciences of the Czech Republic, Flemingovo nám. 2, 16610 Prague 6, Czech Republic,*

[b]*Institute of Chemical Technology, Department of Physical Chemistry, Technická 5, 16628 Prague 6, Czech Republic,*

[c]*J. Heyrovský Institute of Physical Chemistry, Dolejškova 3, 18223 Prague 8, Czech Republic,*

[d]*Helmholtz-Zentrum Berlin für Materialien und Energie, and BESSY, Albert-Einstein-Strasse 15, D-12489 Berlin, Germany,*

[e]*Department of Chemistry, University of Southern California, Los Angeles, California 90089-0482, USA.*

[*]*Corresponding author: petr.slavicek@vscht.cz*

Abstract

We use photoelectron emission spectroscopy with vacuum microjet technique and quantum chemistry calculations to investigate electronic structure and stability of aqueous phosphate anions. Based on the measured photoelectron spectra of sodium phosphates at different pH, we report for the lowest vertical ionization energies of monobasic (9.5 eV), dibasic (8.9 eV) and tribasic (8.4 eV) anions. Electron binding energies were in tandem modelled with *ab initio* methods, using a mixed dielectric solvation model together with up to 64 explicitly solvating water molecules. We demonstrate that two solvation layers of explicit water molecules are needed to obtain converged values of vertical ionization energies (*VIE*s) within this mixed solvation model, leading to very good agreement with experiment. We also show that the highly charged PO_4^{3-} anion, which is electronically unstable in the gas phase, gains the electronic stability with about 16 water molecules, while only 2-3 water molecules are sufficient to stabilize the doubly charged phosphate anion. We also investigate the effect of ion pairing on the vertical ionization energy. In contrast to protonation (leading to a formation of covalent O-H bond), sodiation (leading to an anion..Na^+ ion pair) has only a weak effect on the electron binding energy.

I. Introduction

Isolated molecular anions, especially the multiply charged anions are often intrinsically electronically unstable,[1-4] i.e. the Coulomb repulsion between the extra electrons lead to a spontaneous electron detachment in the gas phase. Many common multivalent anions such as sulphate SO_4^{2-} or carbonate CO_3^{2-} can thus not be isolated in the gas phase, although examples can be found in which molecular anions are stabilized (at least kinetically) by repulsive Coulomb barrier[3] or via spatial separation of the negative charges.[5] Typically, however, the anion stabilization is achieved by means of intermolecular interactions, either with solvent molecules in a solution or with the counterions in a crystal.

Photoelectron spectroscopy is an excellent experimental tool for addressing the question of electronic stability. This technique has indeed been used to study, e.g., doubly charged sulphate anion solvated with 4 to 40 water molecules.[6, 7] Such cluster data can be in principle used for extrapolation either to the condensed phase[8, 9] or in the direction of the (unstable) isolated ion.[10] Direct experimental characterization of solutes in bulk liquid water with photoelectron spectroscopy is, however, a challenging experimental problem which has only relatively recently been addressed using the technique of liquid microjets.[11-13] Prior to this breakthrough, only photoemission thresholds could be estimated for the bulk liquid.[14]

In this contribution, we use vacuum liquid microjet photoelectron spectroscopy combined with extensive *ab initio* calculations to study the solvation effects on the electronic stability of phosphates $H_2PO_4^-$, HPO_4^{2-} and PO_4^{3-} (see Fig. 1). The singly charged dihydrogen phosphate anion is stable already in the gas phase[15] while the doubly and triply charged anions require bound solvent molecules for their existence.[16] Protonation thus significantly changes the electronic stability of the phosphates in the gas phase, which leads to the following question: how do solvating water molecules stabilize the different protonation states and does the protonation change the electron stability also in the bulk liquid? It is also well known that ions, except at low dilution, do not exist in solution as freely solvated species due to their tendency to associate with counterions.[17] This ion pairing becomes more pronounced with increasing charge of the anion and it also strongly depends on the ionic strength.[18] Evidence for ion association can be found in Raman and IR spectroscopy if a molecular anion is probed.[19]

For a triply charged phosphate anion, the unassociated anion will be a very minor species already at very low concentrations and it will vanish at > 0.1 M molar concentrations employed in the photoelectron experiment. We should, therefore, also ask to what extent the electronic stability is affected by the counter-ions or, equivalently, whether counter-ion effects influence the photoemission energetics.

From a practical standpoint, phosphate anions are the basis of the dominant cellular buffer; at pH=7 the anion is almost equally speciated between phosphate in its monovalent ($H_2PO_4^-$) and divalent (HPO_4^{2-}) forms. Also, the negatively charged phosphate backbone is an important component of nucleic acids. The knowledge of phosphate ionization energies (*IE*) is crucial in this context in assessing radiation damage and charge transfer between the nucleic acid components.[20-22] It turns out that the vertical ionization energies of the phosphate moiety and the aromatic bases of DNA are very close to each other.[20, 23, 24] Therefore, it is important to establish the factors that influence the ionization energies at these sites.

Several particular issues concerning the electronic structure and stability of phosphate anions have been addressed in previous studies. Wang et al.[25] have used photoelectron spectroscopy to measure the vertical ionization energy (*VIE*) of an isolated singly charged phosphate anion, $H_2PO_4^-$, reporting a value of about 5 eV. Based on *ab initio* calculations, Boldyrev et al. have argued that triply charged phosphate anion is unstable with respect to the energy loss in the gas phase[15] but the anion can be stabilized in water.[16] Delahay studied photoemission from aqueous phosphate solutions in the 1980s,[14] reporting the onsets of the photoemission at 9.23, 8.79 and 7.44 eV for $H_2PO_4^-$, HPO_4^{2-} and PO_4^{3-} anions.[26] Phosphate anions were also studied by means of photoelectron spectroscopy in the solid state revealing a similar ordering in the lowest VIE for the three differently protonated phosphate forms.[27] Structural properties of phosphate anions in liquid water have been also investigated by means of Raman spectroscopy,[28, 29] electrospray,[30] quantum chemistry calculations[31-34] and *ab initio* and molecular dynamical simulations.[35-37] In these studies, it was shown that phosphate anion is surrounded by a flexible first solvation layer formed according to neutron scattering experiments[38] by 15±3 water molecules. Particular attention was paid to the energetics of different protonation states in the context of pK_a calculations.[39-41] It follows from these studies that the properties of the phosphate anions are controlled by solvation but it is at the same time very difficult to describe the solvation effects on the multiply charged phosphates properly. The fundamental quantity characterizing ion solvation, the hydration energy, has

been reported for PO_4^{3-} with large variations[42, 43] which reflects the ill-defined concept of solvation energy for a species, which does not exist in the gas phase.

The current work combines liquid-phase photoelectron experiments with *ab initio* calculations. We first present the photoelectron spectra recorded for sodium phosphate in different protonation states and these data are then interpreted with calculations. The combination of experiment and calculations allows us to address quantitatively issues concerning the effects of protonation and pairing with counter-ions on the *VIE* and the convergence of electronic stabilization of phosphate anions with the number of solvating water molecules.

II. Methods

II.1 Experimental: Photoemission Measurements

Valence photoelectron-spectroscopy measurements were performed from a 21 μm diameter vacuum liquid microjet[12] at the soft-X-ray U41 PGM undulator beamline of BESSY, Berlin. The jet velocity was ~ 40 ms^{-1}. Our sample solutions were kept at 20°C by a refrigerated/heating circulator prior to being pushed through the glass capillary, forming the microjet. The exact temperature of a ~20 μm vacuum jet has not yet been determined experimentally. However, we estimate that the jet temperature at the locus where photoionization takes place is likely somewhat above 3-5°C. This was the value determined by evaporative-cooling modeling[44-46] for a 15-μm water jet and experimentally from analysis of the velocity distribution of evaporating water gas-phase molecules.[47]

Photon energies were typically 200 eV. Electrons were detected normal to both the synchrotron-light polarization vector and the flow of the liquid jet. A 125 μm diameter orifice that forms the entrance to the hemispherical electron energy-analyzer chamber (10^{-9} mbar) is at a 0.5 mm distance from the liquid jet – a short enough distance to assure that detected electrons have not suffered from inelastic scattering with water gas-phase molecules around the small-sized liquid jet.[11, 12, 48] The low 10^{-4} mbar pressure in the main interaction chamber, under jet-operation conditions, is maintained using turbomolecular and liquid-nitrogen cryopumps. At constant analyzer pass-energy of 10 eV the energy resolution is approximately 100 meV, and the energy resolution of the U41 beamline was better than 50 meV (for a 200

eV photon energy). The small focal size (23 x 12 μm^2) of the X-ray beam at the point of interaction with the liquid microjet allows for matching spatial overlap, and limits the contribution from gas-phase components to less than 5% of the total signal. Photoelectron count rates typically range from 10^3-10^4 s^{-1}. Electron binding energies were calibrated against the binding energy of the $1b_1$ molecular orbital of water liquid water[49] and are presented here relative to the vacuum level.

II.2 Aqueous Solutions and Preparation

Solutions of phosphate salts, trisodium phosphate, Na_3PO_4 (Sigma-Aldrich, purity 96%), disodium hydrogen phosphate, Na_2HPO_4 (Sigma-Aldrich, ≥99%), and sodium dihydrogen phosphate, NaH_2PO_4 (Sigma-Aldrich, ≥ 99%) were prepared at 0.4 M and for Na_3PO_4 at two additional concentrations, 0.1 M and 1 M. The super-saturated solution at 1 M Na_3PO_4 was achieved by heating in an 80° C water bath followed by slow cooling over several hours. This is about a factor of two greater than the normal room-temperature solubility. After cooling to room temperature, pH measurements were taken and each solution was thoroughly inspected to ensure there is no precipitation. All pH measurements we made using a Greisinger brand pH-meter, and great care was taken to ensure proper and frequent calibration. Samples were sub-micron filtered prior to injection into the liquid microjet.

In common with other basic polyvalent ions in water, it is important to consider the speciation expected both with respect to sodium counter-ion association and the protonation state.[18,50-52] Speciation curves can be calculated from recent literature stability constants.[53] As an example we show the relative fractions of free and sodium-associated forms of tribasic phosphate in Figure 2. It is noteworthy that over the concentration range we study, the fraction of free PO_4^{3-} ions is very small and even for the dibasic and monobasic phosphate most anions are associated with a counter-ion. Values for the apparent concentrations of the PO_4^{3-}, HPO_4^{2-}, $H_2PO_4^-$, $NaPO_4^{2-}$, $NaHPO_4^-$, and NaH_2PO_4 species in each experimental solution are presented in Table S1 of the Supplementary Information. The computed pH values are consistent with values measured.

II.3 Calculations

We have modeled the ionization process of the hydrated phosphate anions considering three protonation states: PO_4^{3-}, HPO_4^{2-}, and $H_2PO_4^-$. There are two major issues to be addressed – how to model the ionization process and how to model the solvation.

We have calculated the *VIE*s combining different computational techniques. To calculate the first ionization energy, we have employed the second-order Møller-Plesset perturbation theory with a spin projection (PMP2) method,[54] using the aug-cc-pVDZ basis set. In this approach, the spin contamination problem in the ionized species is minimized. The PMP2 method thus provides high quality ionization energies at a reasonable computational cost for neutral systems, cations, and anions.[55, 56] Ionization energies of larger clusters were estimated at the DFT level with the BMK functional[57] and the 6-31+g* basis set. Higher ionization energies (i.e., ionization energies corresponding to the ejection of more tightly bound electrons) were calculated as the sum of the first ionization energy calculated at the PMP2 level and individual excitation energies corresponding to the excitation into the SOMO orbitals in the ionized state (see Figure S2 in SI). The excitation energies were calculated with time-dependent density functional theory (TDDFT) with the BMK functional and 6-31+g* basis set. We have successfully used this approach previously to model photoionization of nucleic acid components, liquid solutions and ion pairs.[23, 58-60] Since the ionization energies of the phosphate anions lie close to each other, we have also performed benchmark calculations with higher level methods (as presented in the Supporting Information).

Aqueous solvation was modelled using three different approaches: i) microsolvation, i.e., gradually adding the solvating water molecules, ii) representing the water as dielectric continuum within the polarizable continuum model (PCM), and iii) using a hybrid model, in which a cluster with explicit water molecules is embedded in the dielectric continuum. The direct microsolvation approach is problematic since a large number of solvating molecules are typically required to obtain a converged value of the ionization energy; it is, however, possible to use such approaches, e.g., within the effective fragment potential scheme.[61, 62] Dielectric continuum approaches perform well provided the solvent response is linear, i.e., the electrical field exerted by the solute is not too strong. This is likely not to be the case for multiply charged anions and, therefore, a “buffer zone” of explicit water molecules is often needed to ”absorb” the strongest impact of the solute. At the same time, the dielectric

continuum takes care of the long range polarization of the solvent which cannot be neglected particularly for multivalent ions.

A reliable description for anion solvation in polar solvents is a challenging problem in theoretical chemistry. Dielectric continuum models are developed for neutral molecules where short range contribution to the hydration energy is not too important. For anions, the dielectric models perform rather poorly unless the solute cavities are chosen to be artificially small. Augmented dielectric schemes aimed specifically for anions have also been suggested.[63, 64] It has also been reported that some protocols based on the dielectric continuum perform better for ions (and, importantly, also for solute-clusters).[65] These attempts are, however, primarily focused on description of singly charged anions. The theoretical description of phosphate solvation for differently charged anions was a subject of numerous studies in the context of pKa calculations.[39-41] It is found that especially for the doubly and triply charged systems the performance of the dielectric models is rather unsatisfactory, even though one can reach thermodynamical quantities close to the experiment by a proper combination of electronic structure method, dielectric scheme, cavity radius and number of water molecules explicitly considered (see e.g. ref. [41]). The reliability of the solvation modeling is also difficult to assess as the experimentally available single ion properties are also problematic. For example, the "experimental" solvation energy of PO_4^{3-} anion[43] was calculated from a thermodynamical cycle involving lattice energy (calculated with Kapustinski equation[66]) and free energy for crystal dissolution. The calculated value thus corresponds to a virtual species which has the same electronic structure as in the crystal.

The above considerations leads to a conclusion that dielectric continuum or hybrid models with small number of explicitly solvating water molecules will not reliably model the phosphate solvation. We have, therefore, used a "brute force" approach in which we have increased number of explicitly solvating molecules such that the calculated quantities are fully converged and independent of the particular dielectric model used.

The clusters needed for calculations of the ionization energy within the microsolvation and hybrid approaches were generated in two ways. For clusters with less than 6 explicit waters, i.e., $H_iPO_4^{i-3}.(H_2O)_{0-6}$, i = 0-2, we have optimized the ground state geometry at the MP2/aug-cc-pVDZ level in the gas phase and re-optimized the resulting geometry in the PCM continuum within the hybrid model. Large clusters can appear in a great number of

conformations with different ionization energies[67] and the ground state geometries of larger clusters containing up to 64 water molecules were therefore sampled by a density functional-based Born-Oppenheimer molecular dynamics (BOMD). To this end, in order to obtain reasonable starting orientations of water molecules around the anions, we used first classical molecular dynamics simulations with an empirical potential. Partial charges for ions were obtained from *ab initio* calculations, while the rest of the parameters were taken from the OPLS force field.[68] The anion was placed in a cubic box of 25 x 25 x 25 A^3, which was filled by about 500 TIP4P[69] water molecules. The simulation was run for 2 ns at 300 K and 1 atm employing periodic boundary conditions. From the last frame of the trajectory, we cut a cluster containing the anion in the center and 64 or 83 surrounding water molecules. Such geometries served as the initial configuration for BOMD, where dynamics is started after a hundred minimization steps, in order to allow the structure to relax locally.

All BOMD simulations were performed using the mixed Gaussian and plane wave approach, in which the Kohn-Sham orbitals are expanded into Gaussian functions, while for electron density a plane wave basis set is used. We utilized a triple zeta Gaussian basis set augmented with two polarization functions (TZV2P)[70] and Goedecker-Teter-Hutter norm-conserving pseudopotentials[71] for the oxygen and phosphorus core electrons. The PBE exchange-correlation functional[72] empirically corrected for dispersion interactions[73] was used. The system was placed in a 25 x 25 x 25 $Å^3$ cubic box and a cut-off of 280 Ry was used for auxiliary plane-wave basis set. The Poisson equation was treated with a wavelet based solver with open boundary condition,[74] which are adequate for the isolated system. Classical equations of motion were integrated with a time step of 0.5 fs. Canonical sampling through velocity rescaling was used for adjusting the temperature at 250 K. The temperature was set slightly lower than at the ambient conditions in order to suppress evaporation of water molecules from the cluster. Additional runs were performed at 280 K in order to test how much such a temperature change affects the results. In each run, data were accumulated for 7 ps after an equilibration period of 3 ps. Structures for calculation of ionization energies were obtained from these trajectories with a sampling period of 0.25 ps. Clusters smaller than those containing 64 water molecules were obtained by cutting out the most distant water molecules from the central anion.

*VIE*s for the fully optimized small clusters were evaluated at the PMP2/aug-cc-pVDZ level employing the non-equilibrium PCM approach, i.e. taking into account only the optical

part of the polarization while neglecting the nuclear or orientation part. Such approach is consistent with the vertical character of the photoionization process.[20, 23, 55, 56, 60] The *VIE*s of large clusters sampled from the BOMD were calculated at the BMK/6-31+g* level.

In order to check the influence of ion pairing with Na^+ on the *VIE* of the various phosphate forms, we also optimized the $Na_jH_iPO_4^{i+j-3}$, $i + j \leq 3$ clusters in the gas phase, as well as re-optimized them in the PCM solvent and calculated the *VIE* at the PMP2/aug-cc-pVDZ level. Further, we also employed the hybrid model for $NaPO_4^{2-}$, $Na_2PO_4^-$, $NaHPO_4^-$, prepared in the same way as for the unpaired anions. The only adjustment was the fact that a 400 Ry was used for auxiliary plane-wave basis set to properly describe the 8 electrons of Na^+ not included in the pseudopotential.

All BOMD simulations were performed using the mixed Gaussian and plane wave code CP2K/Quickstep,[75] while the classical MD simulations were done using the program package Gromacs.[76] The ionization calculations were performed in Gaussian09 suites of programmes,[77] using the Gaussian03 parameters for the PCM calculations.

III. Results and Discussion

III.1 Experiment

Figure 3 presents valence photoelectron (PE) spectra from aqueous phosphate solutions measured at 200 eV photon energy. All traces are differential spectra, where we have subtracted the water reference solution PE spectrum, which was acquired repetitively in between measurements of the various phosphate solutions. Here we assume that solute and solvent contributions are essentially additive; specific effects on the water electronic structure are usually barely detectable as was observed in our previous studies from a series of electrolyte solutions (e.g., ref. [13]). Signal intensities in Figures 3 are presented as to yield the same height of maximum-intensity peaks, and energies correspond to binding energies relative to vacuum.

PE spectra as a function of protonation state, obtained from 0.4 M NaH_2PO_4 (monobasic), Na_2HPO_4 (dibasic), and Na_3PO_4 (tribasic) starting solutions are shown in Figure 3A. We refer the reader to Table S1 in the Supporting Information as to the expected speciation for these salts in aqueous solution. We find that solutions with the tribasic form of phosphate have the lowest ionization energy, resulting in a PE peak-maximum at 8.4 ± 0.1eV,

and an ionization onset at approximately 7.2-7.3 eV Both values were determined from Gaussian fits of the differential spectra. We defined the ionization onset to five percent of the peak-maximum. Our value agrees well with the threshold energy of 7.44 eV in ref. [14]. For comparison, the position of the lowest ionization-energy peak and onset for neat water is 11.16 and 9.9 eV, respectively.[49] As we increase the protonation state, first with dibasic phosphate the lowest *VIE* increases, leading to a peak maximum at 8.9 ± 0.1 eV, and onset energy at approximately 7.7 eV. For monobasic phosphate these same ionization parameters are at even higher energy, 9.5 ± 0.2 and 8.4 eV, respectively. The 9.5 eV peak position cannot be determined with the same accuracy though as for the other two solutions because there is considerable spectral overlap with the lowest-ionization ($1b_1$) peak from water which has been subtracted; this is also the reason for the larger scatter in signal for *BE* > 10 eV. Unlike for the tribasic phosphate, the onset energy for the dibasic and monobasic forms determined here are approximately 1 eV lower than observed in total-electron-yield threshold experiments.[14] Gaussian functions fitted to the lowest binding energy peaks in Figure 3 yield full width at half maximum of 1.0–1.2 ± 0.1 eV for all three solutions.

The major observed trend for the *VIE* is in agreement with initial expectation, that the more deprotonated the anionic species, the lower the binding energy of the HOMO with a shift from tribasic to monobasic ~1 eV. We will below examine this expectation more carefully theoretically and show how the experimental PE energies, and their distribution (peak widths) compare with calculation. We next observe that the valence PE spectrum from tribasic phosphate exhibits a second peak, at approximately 9.9 eV BE, and a corresponding peak is not observed in the spectra for the dibasic and monobasic forms. However, given the spectral overlap with the water $1b_1$ peak, for the di- and mono- basic forms, we cannot fully rule out some smaller solute-derived intensity in the 10-11 eV *BE* region. The origin of this second peak is not yet fully worked out (see below) but we can exclude that it arises from the OH^-(aq) in equilibrium with the tribasic phosphate; the OH^- ionization energy in water is lower, at 9.2 eV[78] and has an order of magnitude lower concentration than the species giving rise to the main bands (see Supplementary Information).

The concentration dependence of the tribasic valence PE spectra is shown in Figure 3B. The result is illustrated with 0.1, 0.4 and 1.0 M Na_3PO_4 aqueous solution. One might have expected to see a similar binding energy shift to high BE with increasing fraction of counter-ion associated species suggested in Figure 2 (thus reducing the effective charge on the ion in a

similar way to protonation). However, beyond a clear diminishment in the signal to noise, the observed spectral changes are rather minor with the main peak positions not changing. Apparently, the valence band photoelectron spectrum is not sensitive to the association state of the cation, or at least discernible within the scale of the peak broadening. There are subtle changes in the depth of the valley between the two major peaks but this can be satisfactorily explained (see Figure S1 in the supplemental information) by considering the changes in relative fractions of the minor species, OH^- and HPO_4^{2-} present. The effect on the ionization energy of a counter-ion binding and how it differs from protonation will be explored theoretically below.

III.2 Calculations

The presentation of our calculated data follows the structure of Figure 1. We first discuss the stability of the HOMO electron in the triply charged phosphate anion, PO_4^{3-}. This ion is considered as the parent ion from which the other species are derived either by protonation (hydrogenphosphates) or by sodiation. In the experiment, protonation can be controlled by pH and sodiation can be modulated in principle by total concentration. However, note that at the concentrations pertinent to the present experiments the triply charged ion is practically always paired with at least one sodium cation. Finally, we focus on ionization from lower lying electrons.

Ionization of the triply charged phosphate anion (PO_4^{3-})

In the context of the mechanism of aqueous solvation, the triply charged phosphate tri-anion PO_4^{3-} is the most interesting species among the investigated phosphate anions due to the large electric field exerted by the anion on the neighboring water molecules. Such highly charged species polarizes its environment well beyond the linear regime, leading also to a significant amount of charge transfer. Even though Mulliken analysis predicts virtually no charge transfer, other physically more relevant population analysis schemes such as Bader analysis or CHelpG analysis show that 0.7–1.0 e is transferred to the solvent.

The triply charged anion PO_4^{3-} does not exist *per se*. More precisely, the trivalent anion is not supported as an isolated species and a significant number of water molecules are needed to stabilize it against a spontaneous electron detachment. Following our calculations

of clusters of increasing size (the smallest clusters shown in Figure S4 of SI) we find that the smallest cluster containing a stable PO_4^{3-} anion has about 16 water molecules.

Figure 4 and Table 1 show the calculated ionization energies for gas phase clusters containing at least 16 water molecules (where the vertical ionization energy (*VIE*) gains positive values) and for the $PO_4^{3-}(H_2O)_{0\text{-}64}$ clusters embedded in a polarizable dielectric continuum. Adding additional solvent molecules leads to further stabilization of the trianion and, consequently, to the gradual increase of the *VIE*. Still, for the cluster with 64 water molecules the *VIE* is less than 5 eV, i.e., more than 3 eV below the experimental value for Na_3PO_4 solution (Figure 4).

Clearly, the long-range polarization plays an important role in the trianion stabilization. However, using the continuum dielectric model is not sufficient due to strong polarization effects. The *VIE* for the bare phosphate trianion in non-equilibrium PCM is calculated to be only 6.9 eV, which is still more than 1.5 eV below the experimental value. The calculated *VIE* furthermore strongly depends on the size and construction of the cavity used in the PCM calculations. This observation is analogous to the strong dependence of calculated acidity constants on the solute cavity found for triprotic acids.[41] The study of Stefanovich et al.[16] the calculated binding energy with the GCOSMO model for the PO_4^{3-} anion was remarkably close to the experiment. The agreement, however, likely results from error cancelation as the reaction field ought to be considered as completely frozen upon the ionization (neglecting the optical part of the polarizability). We conclude that dielectric models are not able to reliably describe the ionization process for the triply charged phosphate anion.

In order to improve the description, we have thus gradually solvated the trianion by explicit water molecules, embedding the whole system in the dielectric continuum. The *VIE* only slowly increases with the size of the explicit water zone, starting to level off for clusters with more than 50 water molecules, which roughly corresponds to the first two solvation layers. We thus conclude that for the triply charged phosphate anion, a buffer zone of at least two solvation layers is needed before the response of the environment to the ionization can be described within a polarizable continuum.

The triply charged species represents an extreme case of ion solvation. In the following paragraphs, we will consider phosphate anions with lower density of the negative

charge. We follow two routes to decrease the excess negative charge: 1. Protonation leading to the hydrogen-phosphate (HPO_4^{2-}) or dihydrogen-phosphate ($H_2PO_4^-$) anion. A covalent bond between the oxygen and the hydrogen atoms is formed in this case. 2. Sodiation forming ion pairs like $NaPO_4^{2-}$ or $Na_2PO_4^-$. In this case, the sodium cation interacts with the phosphate anion purely via electrostatic interaction.

Protonated phosphate anions: hydrogen-phosphate and dihydrogen-phosphate

As the triply charged PO_4^{3-} anion, the hydrogen phosphate anion HPO_4^{2-} does not exist as an isolated stable anion either. However, just two water molecules are enough to bring the anion the stability leading to positive *VIE* (see Figure S5 of SI for clusters of increasing size). This observation is generally consistent with what is known for other similar divalent anions, such as SO_4^{2-} or $C_2O_4^{2-}$.[3]

Figure 5 and Table 1 show the dependence of the *VIE* of the HPO_4^{2-} anion on the water cluster size, both for the clusters in the gas phase and for the clusters embedded in the dielectric continuum within the hybrid method. The *VIE* of the gas-phase clusters increases upon adding water molecules, reaching the value of about 6 eV for the largest clusters considered (n = 64). There is, however, no indication that the *VIE* is leveling off at this cluster size and the calculated ionization energy is far from the experimental value of 8.90 eV measured for the Na_2HPO_4 solution. The two explicit solvation layers are simply not enough to fully capture the effect of the solvent on the ionization process.

Figure 5 also shows that a dielectric continuum model alone also fails to perform satisfactorily; the *VIE* calculated using PCM is 7.2 eV, i.e., 1.7 eV below the experimental value. One can approach the experiment only by combining the relatively large inner explicit water zone to account for the local polarization effects with the outer dielectric continuum accounting for the long range polarization. It is remarkable that two solvation layers still need to be considered explicitly even though the system charge is smaller than that of the phosphate tri-anion. The resulting *VIE* using the hybrid approach of 9 eV is in an excellent agreement with the experimental value.

The monovalent phosphate anion $H_2PO_4^-$ is stable already as a gas phase species.[25] The experimental gas-phase ionization energy was measured to be 5.1 eV,[25] which is perfectly reproduced at the BMK/aug-cc-pVDZ level. In the gas phase we, nevertheless, experience

some problems with wavefunction stability, leading to a less reliable estimate at the PMP2 level of 5.8 eV. Fortunately, this problem does not occur when water molecules are present (the electronic wavefunction is also stable for other phosphate species).

The *VIE* changes monotonously with the increasing cluster size for the isolated water clusters (save for smallest clusters structures, which were minimized and which are shown Figure S6 of SI). For the largest clusters investigated (i.e., two solvation layers), the mean *VIE* is about 8.5 eV, but again we do not see any sign of convergence (Figure 6 and Table 1). In comparison, the dielectric continuum model performs rather satisfactorily for the singly charged species. For the isolated anion embedded in the dielectric continuum, the *VIE* was calculated to be 9 eV, which is already rather close to the experimental value of 9.5 eV, with the error within the full width at half maximum (FWHM) of the experimental spectrum. The hybrid model further improves the agreement with experiment. The *VIE* within the first solvation layer oscillates around 9 eV but once we include the second solvation layer into the hybrid model, we end up at the *VIE* of 9.6 eV, which practically coincides with the experimental value.

Sodiation of the triply charged anion

Let us now address the question whether the electronic structure of the phosphate anion can be controlled not only via the covalent bonding with a proton but also via the ionic interactions with the sodium counterions present in the solution. For a wide concentration range, the major species in the sodium phosphate is not the bare tri-anion but actually a mixture of the sodiated ($NaPO_4^{2-}$) and disodiated ($Na_2PO_4^-$) anion, see Fig. 2. Investigation of the effects of the sodium phosphate speciation is, therefore, important not only from the conceptual perspective (i.e., what is difference between covalent and ionic bonding in solution) but also in order to correctly interpret the experiment.

Below, we consider systems embedded in the dielectric continuum since in the context of sodiation we are primarily interested in the solution phase chemistry. To gain a quick insight, we have first calculated the *VIE* for the PO_4^{3-}, $NaPO_4^{2-}$ and $Na_2PO_4^-$ anions immersed in the dielectric continuum. The *VIE* for these three clusters are very close to each other, i.e., 6.9 eV PO_4^{3-}, 7.1 or 6.6 eV for $NaPO_4^{2-}$ (depending on cluster geometry), and 6.7 or 6.8 eV for $Na_2PO_4^-$ (depending on cluster geometry); see Figure S7 of SI for isomer geometries. On average, there is no trend with counter-ion number. That is markedly different from what is

observed for the effect of protonation, where the *VIE* changes from 6.9 eV for PO_4^{3-} to 7.2 eV for HPO_4^{2-} and to 9.0 eV for $H_2PO_4^-$. We thus can formulate a hypothesis that sodiation does not strongly influence the *VIE* of the solvated anion. We could, however, be potentially biased by the simple dielectric solvation model used for systems with different charge. We have, therefore, performed also a benchmark simulation of the singly and doubly sodiated phosphate tri-anion solvated with 64 explicit water molecules and then immersed in the PCM. Consistently, the *VIE* remained practically unaffected by sodiation; the *VIE* was calculated to be 8.7 eV for the PO_4^{3-}, 8.6 eV for $NaPO_4^{2-}$, and 8.65 eV for $Na_2PO_4^-$ (the reported values are averages over trajectories performed in the same way as for phosphates without counterions). Similar conclusions as for the sodiation of the triply charged anion can be also drawn for the sodiation of the doubly charged anion. In this case, the mean value of the *VIE* remains ~9.0 eV after counter-ion binding.

Photoelectron spectroscopy of multiply charged ions thus appears rather insensitive (~0.1 eV) to pairing with monovalent counter-ions in solution. The solvent screening effect during the ionization process has been already noticed in our previous studies[20, 23, 60] where the additional screening effect of the counter-ions (on top of that already provided by water) was shown to be small. However, another way to consider this, taking into account the VIE of an isolated Na_3PO_4 molecule (Table 2) which is already within ~1 eV of the aqueous experimental value, is that either counter-ions alone or the solvent alone can provide saturated dielectric stabilization of the anion. The calculated result for isolated Na_3PO_4 is also in line with the XPS data of Gaskell *et al.* where solid state powders of phosphate salts in different protonation states not only shows similar trends to the results here, but also confirm that counter ions alone recover the majority of the stabilization energy.[27]

Ionizations from lower lying molecular orbitals

So far, we have discussed only the lowest *VIE* of the aqueous phosphate ions (corresponding orbitals are shown in Figure S3 of SI). The electrons originating from the lower lying orbitals can, however, also contribute to the experimental PE spectrum. In order to examine their contributions, an indirect approach to calculations of *VIE*s from tighter bound electrons was employed. Namely, the *VIE* originating from ionizing deeper lying electrons is calculated as a sum of the lowest *VIE* and the TDDFT excitation energy of such

electrons to the SOMO orbital of ionized species.[23, 59, 60] This scheme is shown in Figure S2 of the Supporting Information.

According to the TDDFT/NEPCM description (without explicit waters), the first two excitation energies of $PO_4^{2-\cdot}$ radical anion are lower than 0.09 eV, meaning that the first three *VIE*s of PO_4^{3-} are energetically almost degenerate. This could potentially indicate problems with utilizing single-reference methods. However, we have checked the TDDFT results (for gaseous species) against various multireference methods (CASSCF, CASPT2 and MRCI) and the agreement was satisfactory (the benchmark calculations are summarized in the Supporting Information). Higher TDDFT/NEPCM states start at 1.4 eV above the first ionization energy of PO_4^{3-}.

When trying to include explicit water interactions with solvating molecules in the first or second solvation interactions layers, we expect that the energy levels of the higher ionized states will follow similar pattern with the number of explicit waters as the lowest state. Computational analysis of the higher ionized states for the explicitly solvated phosphate anions reveals ionizations from the phosphate moieties become entangled with the ionizations of the water molecules in the first solvating shell (see Supporting Information). These observations therefore suggest a possible explanation of the second peak observed in the photoelectron spectrum of the PO_4^{3-} anion (Figure 3). Based on our calculations, and supported by lack of concentration dependence of the observed signal, we can rule out that it results from different association states of the core PO_4^{3-} anion with different numbers of Na^+ cations. Similarly, the signal cannot be explained as resulting from OH^- anions present in the solution (see simulated spectra in Figure S1 of SI). We, therefore, speculate that the separated and intense second peak at 9.9 eV may correspond to HOMO-*n* ionizations sitting on top of a weaker ionization background from water delocalized orbitals. While the lowest ionized state originates purely from the phosphate moiety, the higher states have increasingly a mixed character involving the neighboring water molecules. Judging from the raw experimental spectra (prior to subtracting the water signal) the involvement of water orbitals can reduce the cross sections by up to a factor of two (see Figure S11 and caption). Further, the calculations support the absence of a second distinct peak within the < 11 eV binding energy experimental window for dibasic and monobasic phosphate (Figure S9 and S10). However, with the present computational methodology, which lacks computation of relative cross sections, we are not able to fully quantitatively resolve this issue.

IV. Conclusions

In this paper, we report photoelectron spectra for aqueous solutions of sodium salts of phosphate anion in its three protonation states, namely dihydrogen phosphate ($H_2PO_4^-$), hydrogen phosphate (HPO_4^{2-}) and phosphate (PO_4^{3-}). We have extracted HOMO electron binding energies which can be attributed to these three anions. We should however emphasize that at the relatively high electrolyte concentrations used in our study, the measured binding energies correspond mostly to the ion pairs of the anions with the sodium counterions. We also model the electronic structure of solvated phosphate anions by means of *ab initio* methods and the calculations are used to interpret the photoemission experiment. The major conclusions can be summarized as follows (for summary of experimental and computational results see Table 2):

1. For the dihydrogen phosphate $H_2PO_4^-$, the binding energy of the HOMO electron increases from 5.06 eV in the gas phase[25] to 9.5 eV. Hydrogen phosphate (HPO_4^{2-}) and phosphate (PO_4^{3-}) anions have never been isolated in the gas phase, due to their electronic instability, but the binding energies in water were measured to be 8.9 eV for HPO_4^{2-} and 8.4 eV for PO_4^{3-}. Liquid microjet photoelectron spectroscopy thus characterizes the electronic stabilization of the anion by the solvent.

2. Based on our theoretical calculations, we estimate that about 16 water molecules are needed to support the electronic stability of PO_4^{3-} while 2-3 water should suffice to support the existence of HPO_4^{2-}.

3. It was possible to reproduce the experimentally reported binding energies (and photoelectron spectra) within the hybrid cluster/continuum approach. However, for multiply charged anions it was necessary to fully solvate the phosphate anion with two layers of explicit water molecules to reproduce the experiment.

4. Our calculations show that the protonation (i.e. formation of covalent bond between H^+ and the anion) increases the *VIE* of phosphate anion, while ion pairing with Na^+ does not influence it due to the screening effect of water. This conclusion is in a full agreement with the experiments for phosphates in different protonation states studied at different electrolyte concentrations.

5. Both experimental and simulated photoelectron spectra exhibit a rather broad peak width (above 1 eV), which can be rationalized as a combination of distribution of solvent and counter-ion structures, as well as vibrational and electronic states of the anion. For the former (inhomogeneous) broadening the current calculations show that the distribution of solvent structures gives the major contribution.

Electron detachment from the phosphate anions leads to the formation of phosphate radicals, $H_2PO_4^{\cdot}$, $HPO_4^{-\cdot}$, and $PO_4^{2-\cdot}$. These highly oxidizing radicals, rapidly reacting with organic compounds in aqueous solutions,[79-81] are often present in high concentrations in industrial waste waters and they can be also involved in biological radiation processes. The redox potentials are not currently available and are presently only estimated based on the radical reactivities.[79] The photoemission measurements described here provide independent estimates of the order and variation in the reduction potentials of phosphate radicals.

The phosphate anion represents an interesting case of a common system which is capable of existence only in a solvated state. Although, unstable with respect to ejection of an electron without hydration, full solvation actually makes the anion electronically more stable than the majority of neutral organic biomolecules (whose VIEs are ~7 – 8 eV).[20, 55] This has an important biophysical consequence. The phosphate moiety is an essential part of the nucleic acid skeleton and a major component by mass of the polymer. Therefore, it is a significant potential target for direct action of ionizing radiation. Importantly, ionizing damage at this moiety would likely lead to a strand break. However, at least for free inorganic phosphate we have established that solvation brings the frontier orbitals into near alignment with those of water. In a separate publication, we address the vertical ionization processes from nucleotides, and will address the relative roles of ionization at the aromatic base, sugar and phosphate centers.

Acknowledgment

PS acknowledges support from the Czech Science Foundation (Grants no. P208/10/1724 and P208/11/0161). Support to PJ from the Czech Science Foundation (Grant 203/08/0114) and the award from the Academy of Sciences (PraemiumAcademie) is gratefully acknowledged. EP and MO acknowledge support from IMPRS Dresden. BW acknowledges support from the

Deutsche Forschungsgemeinschaft (DFG project WI 1327/3-1). CS and SEB acknowledge support from the US National Science Foundation under CHE-0957869 and the award of beam time at Helmholtz-Zentrum Berlin. Additionally, CS received a travel support grant from the USC Provosts Office.

Tables

Table 1 The lowest vertical ionization energy of $H_iPO_4^{i-3}(H_2O)_n$ in solution (hybrid model: combined clusters/NEPCM approach) at the BMK/6-31+g* level. The mean values and half width at half maximum (FHMW/2) calculated from standard deviation of the data set for each cluster size are given in eV.

n	$PO_4^{3-}(H_2O)_n$	$HPO_4^{2-}(H_2O)_n$	$H_2PO_4^{-}(H_2O)_n$
10	7.11 ± 0.26	8.00 ± 0.29	9.06 ± 0.37
16	7.54 ± 0.25	8.15 ± 0.33	9.03 ± 0.36
24	7.80 ± 0.32	8.34 ± 0.36	8.99 ± 0.39
32	7.98 ± 0.41	8.49 ± 0.38	9.21 ± 0.47
40	8.22 ± 0.38	8.63 ± 0.39	9.33 ± 0.43
48	8.45 ± 0.42	8.88 ± 0.45	9.42 ± 0.42
56	8.70 ± 0.48	9.02 ± 0.48	9.52 ± 0.54
64	8.73 ± 0.53	9.10 ± 0.50	9.67 ± 0.51

Table 2 The effect of protonation and ion pair formation on VIEs of phosphate anions. The lowest vertical ionization energy of $Na_iH_jPO_4^{j+i-3}$, $i+j \leq 3$ in the gas phase and in solution modelled within NEPCM as well as hybrid approach with the PMP2/aug-cc-pVDZ method. Different sodiation isomers are presented.

	Tribasic				Dibasic			Monobasic		
	PO_4^{3-}	$NaPO_4^{2-}$	$Na_2PO_4^-$	Na_3PO_4	HPO_4^{2-}	$NaHPO_4^-$	Na_2HPO_4	$H_2PO_4^-$	NaH_2PO_4	H_3PO_4
VIE (NEPCM)	6.90	7.07	6.73	7.77	7.19	7.53	7.90	8.99	9.30	10.52
		6.55	6.84	7.89		7.52				10.50
				7.16						
average	6.9	6.8	6.8	7.6	7.2	7.5	7.9	9.0	9.3	10.5
VIE (hybrid approach)	8.7	8.6	8.65		9.0	9.0		9.65		
VIE (gas phase)	-6.92	-1.80	2.22	7.18	-1.44	3.07	8.73	5.13[a]	10.50	11.77
		-2.22	2.71	7.35		4.22				11.78
			2.88	6.80						
				7.69						
				7.41						
				7.13						
Experiment	8.4 ± 0.1 eV				8.9 ± 0.1 eV			9.5 ± 0.2 eV		-

a) The value of VIE for the gas phase $H_2PO_4^-$ anion was calculated at the BMK/aug-cc-pVDZ level since the HF wavefunction experiences stability problems in this case.

Figure captions

Figure 1: Species derived from the tribasic phosphate anion PO_4^{3-} upon protonation and sodiation (*i.e.*, ion pair formation).

Figure 2: Histogram depicting the room temperature population fractions of sodium associated species for tribasic phosphate solutions of varying overall concentration. (Black) trivalent phosphate, no associated sodium ions; (Red) divalent phosphate, one associated sodium ion; (Green) monovalent phosphate, two associated sodium ions. Equilibrium fractions are estimated based on literature constants for sodium cation association. Speciation calculations are described in Supporting Information; here calculation assumes high pH limit where no protonated forms (dibasic, monobasic) are populated.

Figure 3: Differential valence-photoelectron spectra from phosphate buffered aqueous solutions measured at 200 eV photon energy. (A) From 0.4 M Na_3PO_4 (pH = 12.08), Na_2HPO_4 (pH = 9.33), and NaH_2PO_4 solution (pH = 4.24). (B) From Na_3PO_4 solution at 0.1, 0.4, and 1.0 M concentration. The dashed lines are a guide to the eye to compare tiered spectra. The PE spectrum from 1.0 M concentration (in red) is reproduced in the tiers of the lower concentration measurements.

Figure 4: The lowest vertical ionization energy of $PO_4^{3-}(H_2O)_{16-64}$ in the gas phase (lower part, blue color) and of $PO_4^{3-}(H_2O)_{0-64}$ in solution modelled via hybrid approach (combined clusters/NEPCM) approach (upper part, orange color). In the gas phase, cluster sizes with negative *VIE* were omitted, diamonds represent clusters obtained from BOMD trajectories.

For the hybrid model, *VIE*s of small optimized clusters (containing up to 6 water molecules) calculated at the PMP2/aug-cc-pVDZ level are presented with orange circles. There can be more hydration isomers for each cluster size. Diamonds refer to *VIE*s of clusters containing 10 - 64 water molecules cut from BOMD trajectories calculated at the BMK/6-31+g* level. The mean values are connected with dashed line for a better visualization; the intervals between black bars represent FWHM calculated from standard deviation of the data set.

Experimental photoelectron spectrum of solution containing PO_4^{3-} is shown on the right hand side.

Figure 5: The lowest vertical ionization energy of $HPO_4^{2-}(H_2O)_{2-64}$ in the gas phase (lower part, blue color) and of $HPO_4^{2-}(H_2O)_{0-64}$ in solution modelled via hybrid (combined clusters/NEPCM) approach (upper part, orange color). In the gas phase, cluster sizes with negative *VIEs* were omitted. Blue circles refer to *VIE*s of small cluster (2-6 water molecules) calculated at the PMP2/aug-cc-pVDZ level, there can be more hydration isomers for each cluster size. Diamonds represent clusters cut from BOMD trajectories.

For the hybrid model, *VIE*s of small optimized clusters (containing up to 6 water molecules) calculated at the PMP2/aug-cc-pVDZ level are depicted by orange circles. There can be more hydration isomers for each cluster size. Diamonds refer to *VIE*s of clusters containing 10 - 64 water molecules cut from BOMD trajectories calculated at the BMK/6-31+g* level. The mean values are connected with dashed line for a better visualization; the intervals between black bars represent FWHM calculated from standard deviation of the data. Experimental photoelectron spectrum of solution containing HPO_4^{2-} is shown on the right hand side.

Figure 6: The lowest vertical ionization energy of $H_2PO_4^-(H_2O)_{0-64}$ in the gas phase (lower part, blue color) and in solution modelled via hybrid(combined clusters/NEPCM) approach (upper part, orange color). Blue circles refer to *VIE*s of optimized small cluster (0-6 water molecules) calculated at the PMP2/aug-cc-pVDZ level, there can be more hydration isomers for each cluster size. Diamonds represent clusters cut from BOMD trajectories.

For the hybrid model, *VIE*s of small optimized clusters (containing up to 6 water molecules) calculated at the PMP2/aug-cc-pVDZ level are depicted by orange circles. There can be more hydration isomers for each cluster size. Diamonds refer to *VIE*s of clusters containing 10 - 64 water molecules cut from BOMD trajectories calculated at the BMK/6-31+g* level. The mean values are connected with dashed line for a better visualization; the intervals between black bars represent FWHM calculated from standard deviation of the data set. Experimental photoelectron spectrum of solution containing $H_2PO_4^-$ is shown on the right hand side.

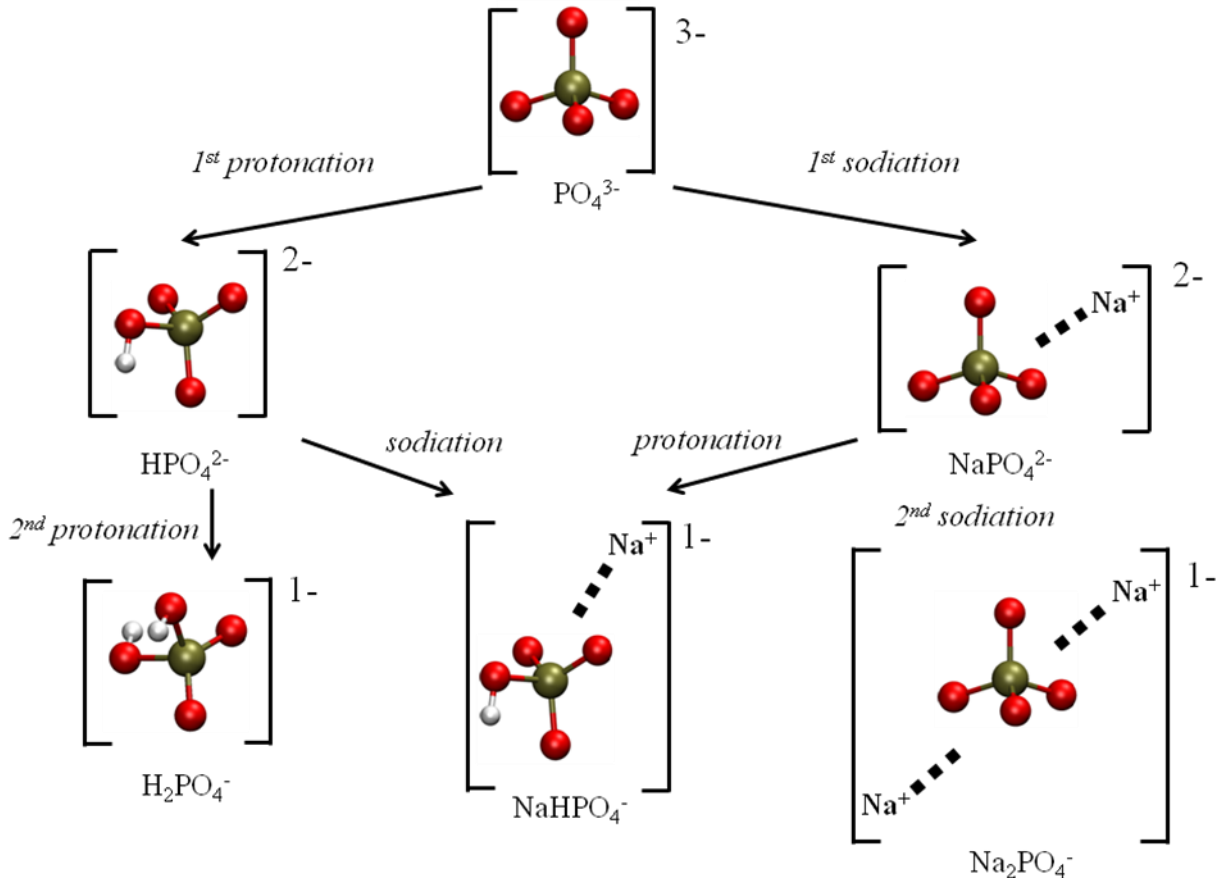
3-
1st protonation
1st sodiation
PO4 3-
2-
Na+
2-
HPO4 2-
sodiation
protonation
NaPO4 2-
2nd protonation
2nd sodiation
Na+
1-
1-
Na+
1-
Na+
H2PO4-
NaHPO4-
Na+
Na2PO4-

Figure 1

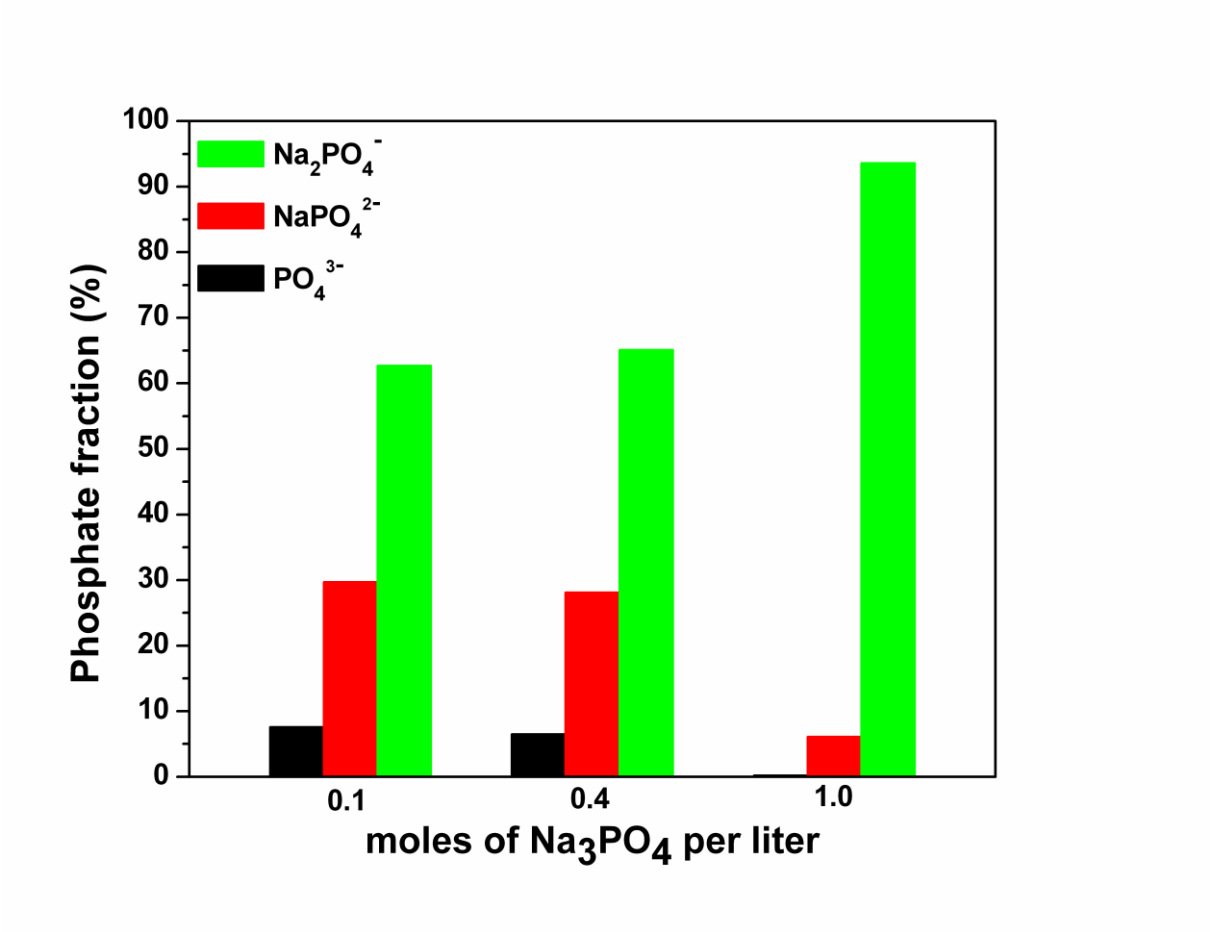
100
90
80
70
60
50
40
30
20
10
0
Phosphate fraction (%)
$Na_2PO_4^-$
$NaPO_4^{2-}$
PO_4^{3-}
0.1
0.4
1.0
moles of Na_3PO_4 per liter

Figure 2

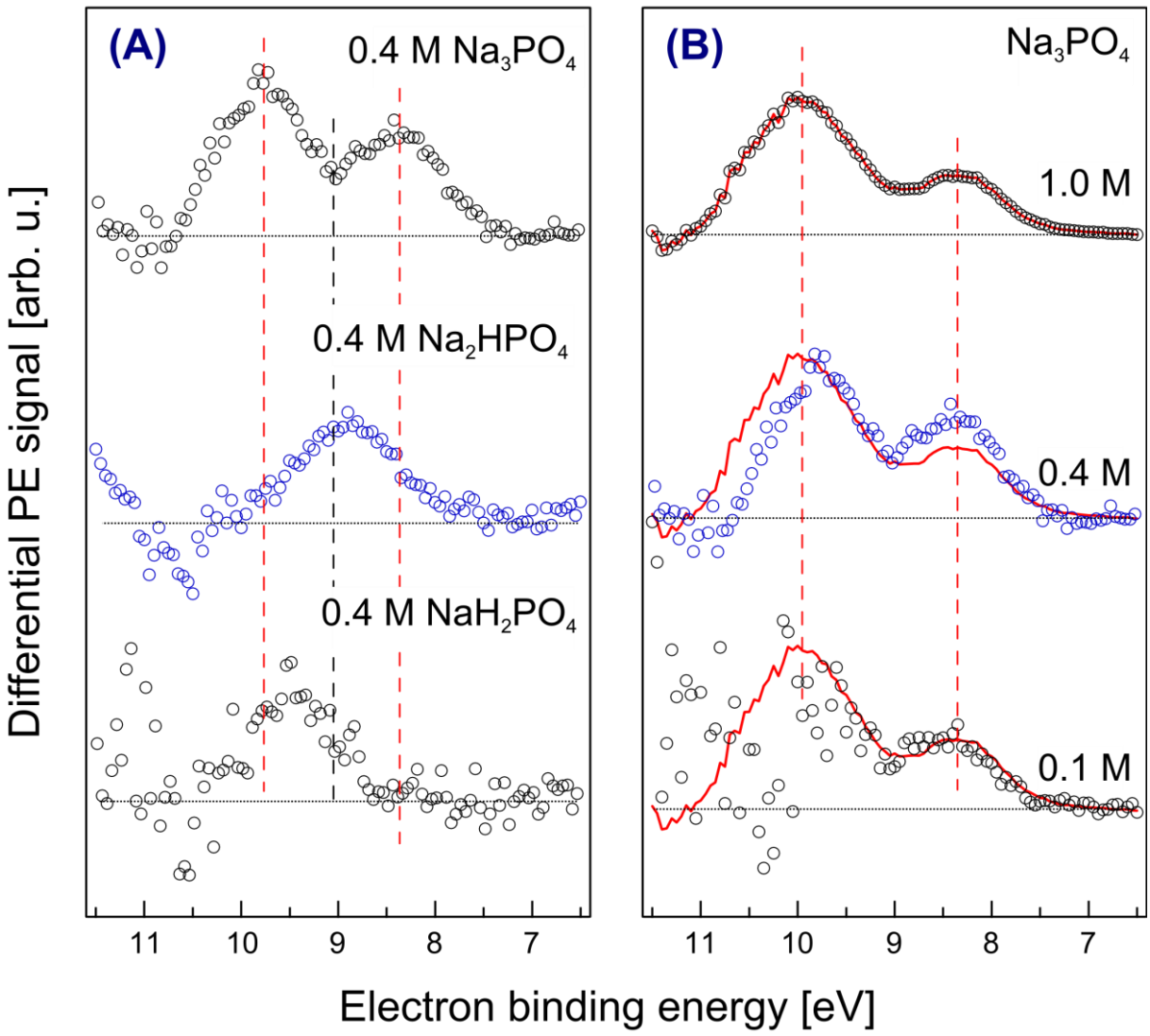
(A)
0.4 M Na3PO4
0.4 M Na2HPO4
0.4 M NaH2PO4
(B)
Na3PO4
1.0 M
0.4 M
0.1 M
Differential PE signal [arb. u.]
11
10
9
8
7
Electron binding energy [eV]

Figure 3

Figure 4

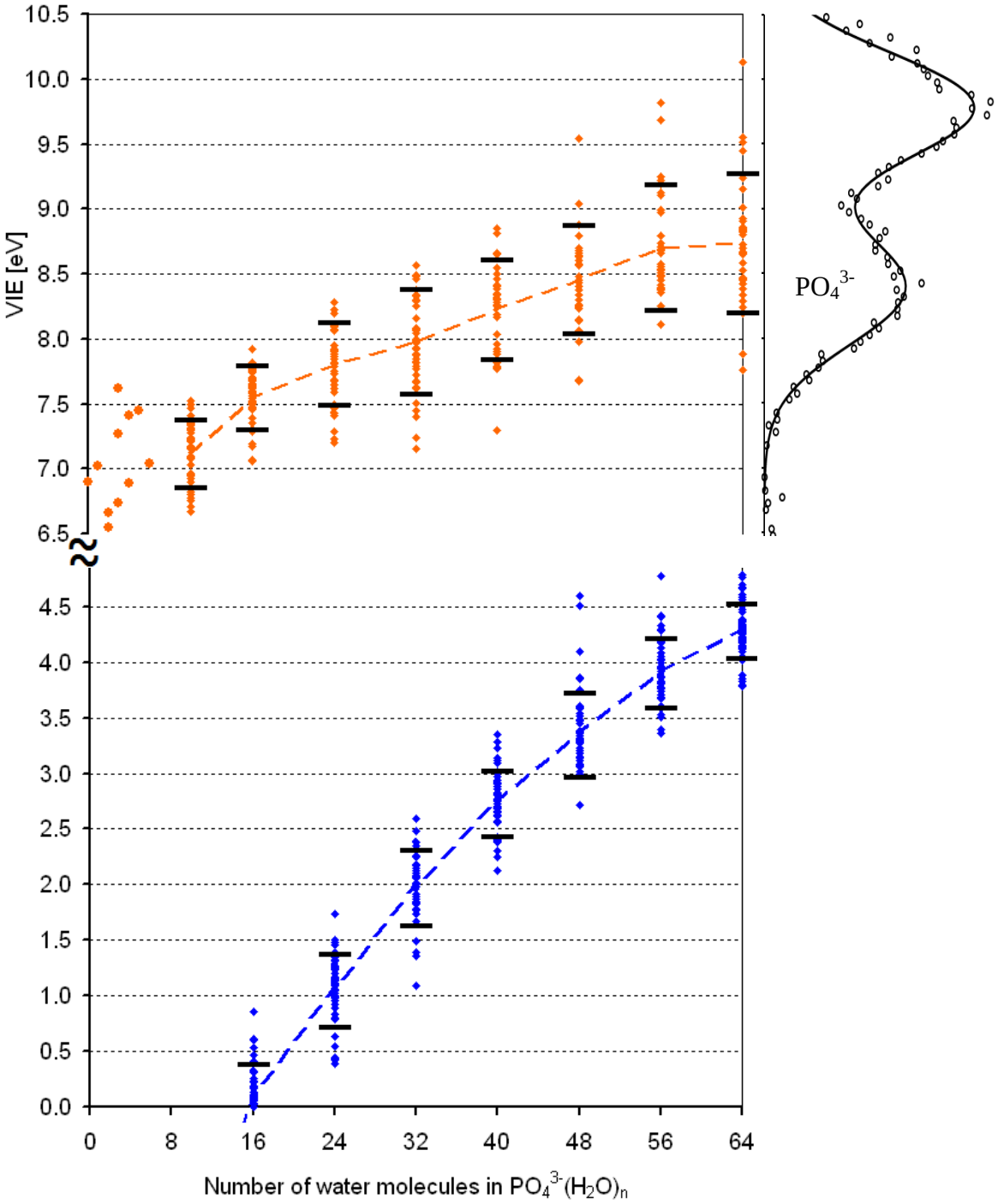
VIE [eV]
10.5
10.0
9.5
9.0
8.5
8.0
7.5
7.0
6.5
4.5
4.0
3.5
3.0
2.5
2.0
1.5
1.0
0.5
0.0
0
8
16
24
32
40
48
56
64
Number of water molecules in $PO_4^{3-}(H_2O)_n$
PO_4^{3-}

Figure 5

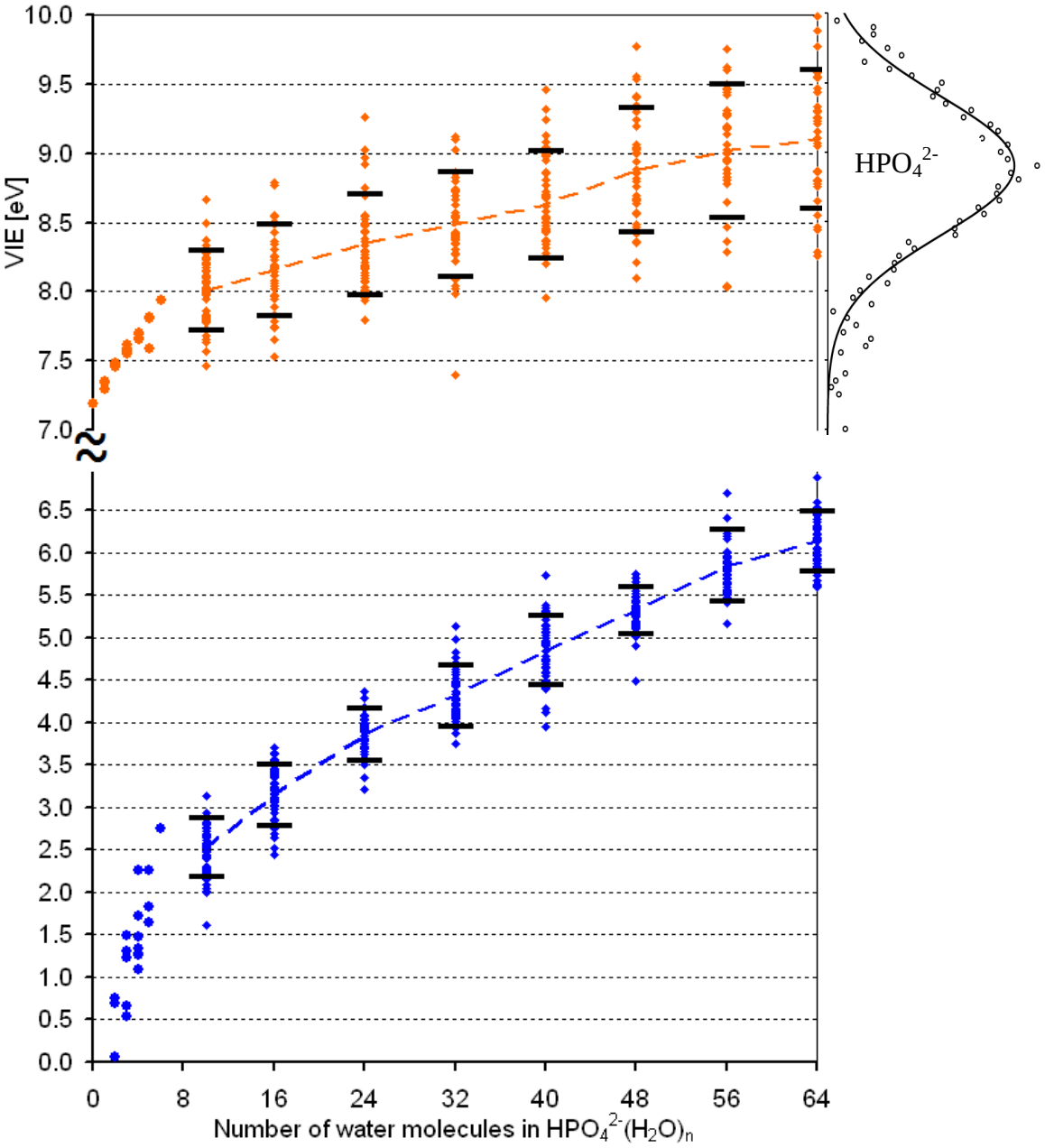
VIE [eV]
10.0
9.5
9.0
8.5
8.0
7.5
7.0
6.5
6.0
5.5
5.0
4.5
4.0
3.5
3.0
2.5
2.0
1.5
1.0
0.5
0.0
0
8
16
24
32
40
48
56
64
Number of water molecules in HPO4 2-(H2O)n
HPO4 2-

Figure 6

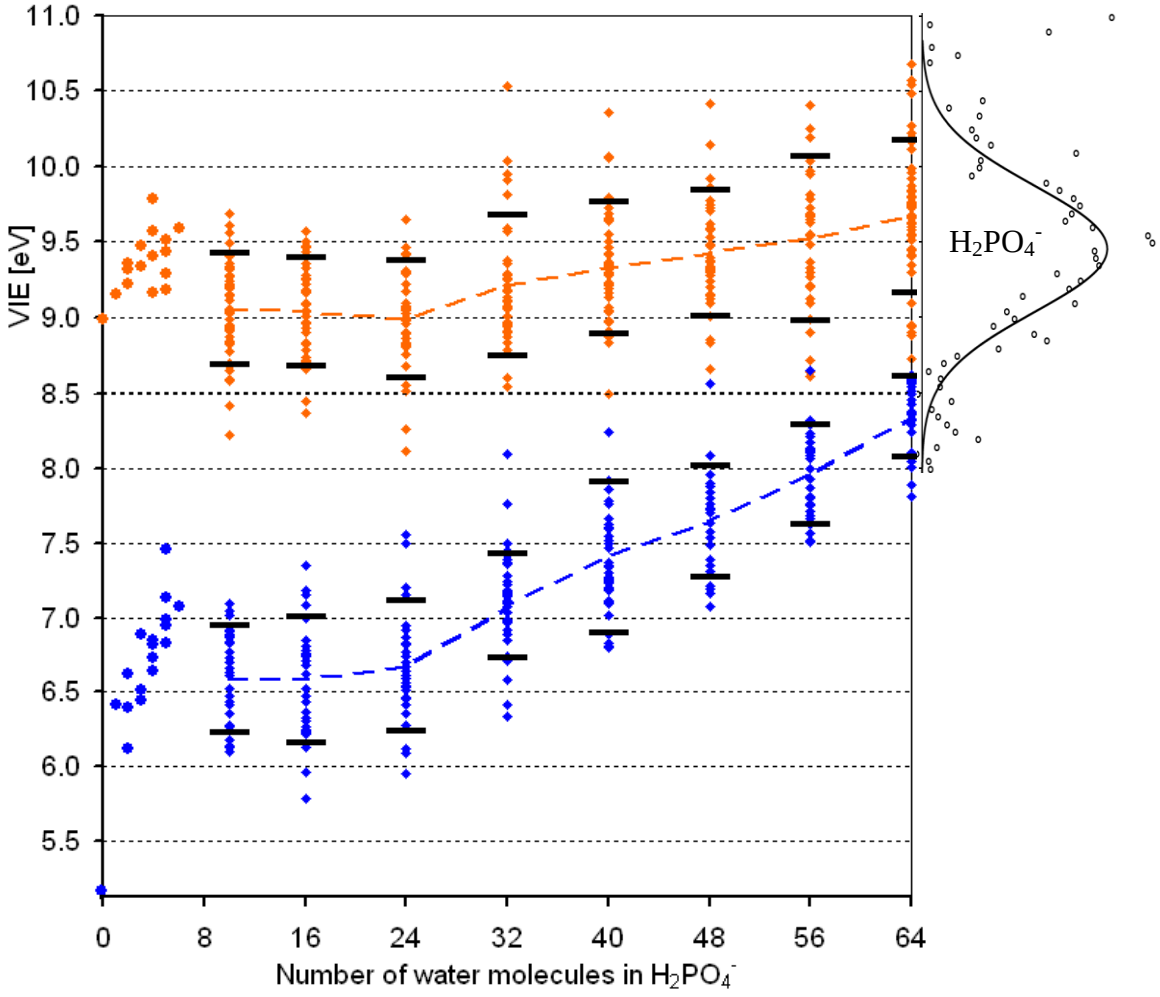
11.0
10.5
10.0
9.5
9.0
8.5
8.0
7.5
7.0
6.5
6.0
5.5
VIE [eV]
0
8
16
24
32
40
48
56
64
Number of water molecules in H2PO4-
H2PO4-

References

1. A. I. Boldyrev, M. Gutowski, J. Simons *Accounts Chem Res* **1996**, *29*, 497.
2. J. Simons *J Phys Chem A* **2008**, *112*, 6401.
3. X. B. Wang, L. S. Wang *Annu Rev Phys Chem* **2009**, *60*, 105.
4. A. Dreuw, L. S. Cederbaum *Chem Rev* **2002**, *102*, 181.
5. X. Yang, Y. J. Fu, X. B. Wang, P. Slavicek, M. Mucha, P. Jungwirth, L. S. Wang *J Am Chem Soc* **2004**, *126*, 876.
6. X. Yang, X. B. Wang, L. S. Wang *J Phys Chem A* **2002**, *106*, 7607.
7. X. B. Wang, X. Yang, J. B. Nicholas, L. S. Wang *Science* **2001**, *294*, 1322.
8. J. Jortner *Z Phys D Atom Mol Cl* **1992**, *24*, 247.
9. A. K. Pathak, A. K. Samanta, D. K. Maity, T. Mukherjee, S. K. Ghosh *J Phys Chem Lett* **2010**, *1*, 886.
10. A. K. Pathak, A. K. Samanta, D. K. Maity, T. Mukherjee, S. K. Ghosh *Phys Rev E* **2011**, *83*.
11. B. Winter, M. Faubel *Chem. Rev.* **2006**, *106*, 1176.
12. B. Winter *Nucl Instrum Meth A* **2009**, *601*, 139.
13. R. Seidel, S. Thurmer, B. Winter *J Phys Chem Lett* **2011**, *2*, 633.
14. P. Delahay *Accounts Chem Res* **1982**, *15*, 40.
15. A. I. Boldyrev, J. Simons *J Phys Chem-Us* **1994**, *98*, 2298.
16. E. V. Stefanovich, A. I. Boldyrev, T. N. Truong, J. Simons *J Phys Chem B* **1998**, *102*, 4205.
17. Y. Marcus, G. Hefter *Chem Rev* **2006**, *106*, 4585.
18. A. E. Martell, R. A. Smith, *Critical Stability Constants: Second Supplement* (Plenum, New York, 1974).
19. J. M. G. Barthel, H. Krinke, W. Kunz, *Physical Chemistry of Electrolyte Solutions* (Steinkopff, 2002).
20. P. Slavicek, B. Winter, M. Faubel, S. E. Bradforth, P. Jungwirth *J Am Chem Soc* **2009**, *131*, 6460.
21. S. Kanvah, J. Joseph, G. B. Schuster, R. N. Barnett, C. L. Cleveland, U. Landman *Accounts Chem Res* **2010**, *43*, 280.
22. H. Fernando, G. A. Papadantonakis, N. S. Kim, P. R. LeBreton *P Natl Acad Sci USA* **1998**, *95*, 5550.
23. E. Pluharova, P. Jungwirth, S. E. Bradforth, P. Slavicek *J Phys Chem B* **2011**, *115*, 1294.
24. C. Schroeder *et al., planned* **2012**.
25. X. B. Wang, E. R. Vorpagel, X. Yang, L. S. Wang *J Phys Chem A* **2001**, *105*, 10468.
26. K. Vonburg, P. Delahay *Chem Phys Lett* **1981**, *78*, 287.
27. K. J. Gaskell, M. M. Smith, P. M. A. Sherwood *J Vac Sci Technol A* **2004**, *22*, 1331.
28. K. A. Syed, S.-F. Pang, Y. Zhang, G. Zeng, Y.-H. Zhang *The Journal of Physical Chemistry A* **2012**, *116*, 1558.
29. C. C. Pye, W. W. Rudolph *J Phys Chem A* **2003**, *107*, 8746.
30. A. T. Blades, Y. H. Ho, P. Kebarle *J Phys Chem-US* **1996**, *100*, 2443.
31. Y. Yang, H. B. Yu, D. York, M. Elstner, Q. Cui *J Chem Theory Comput* **2008**, *4*, 2067.
32. C. Ebner, U. Onthong, M. Probst *J Mol Liq* **2005**, *118*, 15.
33. S. A. Brandan, S. B. Diaz, R. C. Picot, E. A. Disalvo, A. Ben Altabef *Spectrochim Acta A* **2007**, *66*, 1152.
34. M. E. Colvin, E. Evleth, Y. Akacem *J Am Chem Soc* **1995**, *117*, 4357.
35. E. Tang, D. Di Tommaso, N. H. de Leeuw *J Chem Phys* **2009**, *130*.

36. A. B. Pribil, T. S. Hofer, B. R. Randolf, B. M. Rode *J Comput Chem* **2008**, *29*, 2330.
37. J. vandeVondele *J. Phys. Chem., ASAP* **2012**.
38. P. E. Mason, J. M. Cruickshank, G. W. Neilson, P. Buchanan *Phys Chem Chem Phys* **2003**, *5*, 4686.
39. E. Tang, D. Di Tommaso, N. H. de Leeuw *Phys Chem Chem Phys* **2010**, *12*, 13804.
40. M. Smiechowski *J Mol Struct* **2009**, *924-26*, 170.
41. T. B. Lee, M. L. Mckee *Phys Chem Chem Phys* **2011**, *13*, 10258.
42. Y. Marcus *J Chem Soc Faraday T* **1991**, *87*, 2995.
43. P. George, R. J. Witonsky, Trachtma.M, C. Wu, W. Dorwart, L. Richman, W. Richman, F. Shurayh, B. Lentz *Biochim Biophys Acta* **1970**, *223*, 1.
44. M. Faubel, S. Schlemmer, J. P. Toennies *Z Phys D Atom Mol Cl* **1988**, *10*, 269.
45. A. Charvat, E. Lugovoj, M. Faubel, B. Abel *Rev Sci Instrum* **2004**, *75*, 1209.
46. K. R. Wilson, B. S. Rude, J. Smith, C. Cappa, D. T. Co, R. D. Schaller, M. Larsson, T. Catalano, R. J. Saykally *Rev Sci Instrum* **2004**, *75*, 725.
47. M. Faubel, T. Kisters *Nature* **1989**, *339*, 527.
48. M. Faubel, B. Steiner, J. P. Toennies *J. Chem. Phys.* **1997**, *106*, 9013.
49. B. Winter, R. Weber, W. Widdra, M. Dittmar, M. Faubel, I. V. Hertel *J Phys Chem A* **2004**, *108*, 2625.
50. J. R. Van Wazer, C. F. Callis *Chem Rev* **1958**, *58*, 1011.
51. P. Haake, R. V. Prigodich *Inorg Chem* **1984**, *23*, 457.
52. R. V. Prigodich, P. Haake *Inorg Chem* **1985**, *24*, 89.
53. P. G. Daniele, A. Derobertis, C. Destefano, A. Gianguzza, S. Sammartano *J Solution Chem* **1991**, *20*, 495.
54. H. B. Schlegel *J Phys Chem-Us* **1988**, *92*, 3075.
55. B. Jagoda-Cwiklik, P. Slavicek, L. Cwiklik, D. Nolting, B. Winter, P. Jungwirth *J Phys Chem A* **2008**, *112*, 3499.
56. B. Jagoda-Cwiklik, P. Slavicek, D. Nolting, B. Winter, P. Jungwirth *J Phys Chem B* **2008**, *112*, 7355.
57. A. D. Boese, J. M. L. Martin *J Chem Phys* **2004**, *121*, 3405.
58. S. Thurmer, R. Seidel, B. Winter, M. Oncak, P. Slavicek *J Phys Chem A* **2011**, *115*, 6239.
59. O. Svoboda, M. Oncak, P. Slavicek *J Chem Phys* **2011**, *135*.
60. L. Sistik, M. Oncak, P. Slavicek *Phys Chem Chem Phys* **2011**, *13*, 11998.
61. D. Ghosh, O. Isayev, L. V. Slipchenko, A. I. Krylov *J Phys Chem A* **2011**, *115*, 6028.
62. K. Khistyaev, K. B. Bravaya, E. Kamarchik, O. Kostko, M. Ahmed, A. I. Krylov *Faraday Discuss* **2011**, *150*, 313.
63. D. M. Chipman *J Chem Phys* **2003**, *118*, 9937.
64. A. Pomogaeva, D. W. Thompson, D. M. Chipman *Chem Phys Lett* **2011**, *511*, 161.
65. C. P. Kelly, C. J. Cramer, D. G. Truhlar *J Chem Theory Comput* **2005**, *1*, 1133.
66. A. F. Kapustinskii *Q Rev Chem Soc* **1956**, *10*, 283.
67. A. K. Pathak, A. K. Samanta, D. K. Maity *Phys Chem Chem Phys* **2011**, *13*, 6315.
68. W. L. Jorgensen, J. Tirado-Rives *J Am Chem Soc* **1988**, *110*, 1657.
69. W. L. Jorgensen, J. Chandrasekhar, J. D. Madura, R. W. Impey, M. L. Klein *J Chem Phys* **1983**, *79*, 926.
70. J. VandeVondele, J. Hutter *J Chem Phys* **2007**, *127*.
71. S. Goedecker, M. Teter, J. Hutter *Phys Rev B* **1996**, *54*, 1703.
72. J. P. Perdew, K. Burke, M. Ernzerhof *Phys Rev Lett* **1996**, *77*, 3865.
73. S. Grimme *J Comput Chem* **2006**, *27*, 1787.

74. L. Genovese, T. Deutsch, A. Neelov, S. Goedecker, G. Beylkin *J Chem Phys* **2006**, *125*.
75. J. VandeVondele, M. Krack, F. Mohamed, M. Parrinello, T. Chassaing, J. Hutter *Comput Phys Commun* **2005**, *167*, 103.
76. B. Hess, C. Kutzner, D. van der Spoel, E. Lindahl *J Chem Theory Comput* **2008**, *4*, 435.
77. M. J. Frisch, G. W. Trucks, H. B. Schlegel, G. E. Scuseria, M. A. Robb, J. R. Cheeseman, G. Scalmani, V. Barone, B. Mennucci, G. A. Petersson, H. Nakatsuji, M. Caricato, X. Li, H. P. Hratchian, A. F. Izmaylov, J. Bloino, G. Zheng, J. L. Sonnenberg, M. Hada, M. Ehara, K. Toyota, R. Fukuda, J. Hasegawa, M. Ishida, T. Nakajima, Y. Honda, O. Kitao, H. Nakai, T. Vreven, J. A. Montgomery, J. E. Peralta, F. Ogliaro, M. Bearpark, J. J. Heyd, E. Brothers, K. N. Kudin, V. N. Staroverov, R. Kobayashi, J. Normand, K. Raghavachari, A. Rendell, J. C. Burant, S. S. Iyengar, J. Tomasi, M. Cossi, N. Rega, J. M. Millam, M. Klene, J. E. Knox, J. B. Cross, V. Bakken, C. Adamo, J. Jaramillo, R. Gomperts, R. E. Stratmann, O. Yazyev, A. J. Austin, R. Cammi, C. Pomelli, J. W. Ochterski, R. L. Martin, K. Morokuma, V. G. Zakrzewski, G. A. Voth, P. Salvador, J. J. Dannenberg, S. Dapprich, A. D. Daniels, Farkas, J. B. Foresman, J. V. Ortiz, J. Cioslowski, D. J. Fox, Gaussian 09, Revision B.01. Wallingford CT, **2009**.
78. B. Winter, M. Faubel, I. V. Hertel, C. Pettenkofer, S. E. Bradforth, B. Jagoda-Cwiklik, L. Cwiklik, P. Jungwirth *J Am Chem Soc* **2006**, *128*, 3864.
79. P. Maruthamuthu, P. Neta *J Phys Chem-Us* **1978**, *82*, 710.
80. S. Steenken, L. Goldbergerova *J Am Chem Soc* **1998**, *120*, 3928.
81. S. S. Cencione, M. C. Gonzalez, D. O. Martire *J Chem Soc Faraday T* **1998**, *94*, 2933.